BULLETIN DE L'ASSOCIATION MINERALOGIQUE DU CANADA

THE CANADIAN MINERALOGIST

JOURNAL OF THE MINERALOGICAL ASSOCIATION OF CANADA

Volume 35 June 1997 Part 3

The Canadian Mineralogist
Vol. 35, pp. 573-586 (1997)

GOLD–COPPER ALLOY MINERALS FROM THE KERR MINE, ONTARIO

STEPHEN W. KNIPE AND MICHAEL E. FLEET[1]

Department of Earth Sciences, University of Western Ontario, London, Ontario N6A 5B7

ABSTRACT

High-level "green carbonate" ore from the Kerr mine (formerly known as Kerr–Addison mine), Virginiatown, Ontario, contains grains of gold with varying degrees of replacement by copper in a late-stage, low-temperature fluid-mediated event. In reflected light, the gold–copper minerals appear as variably yellow-pink grains, with a moderately lower reflectance, but better polish than pure gold. Au–Cu grains are localized at the margin of pre-existing grains of gold; replacement is more advanced in thin stringer gold. Gold and three Au–Cu phases have been recognized, and characterized by EMPA, and XRD and XPS: phase 1: gold, with minor Ag, Hg and Cu, with the disordered *Fm*3*m* structure (92.6 at.% Au, 6.4% Ag, 0.6% Hg, 0.4% Cu), phase 1b: gold, with variably elevated contents of Ag and Cu (89.9 at.% Au, 7.3% Ag, 0.4% Hg, 2.4% Cu), phase 2: Au_3Cu, with *Fm*3*m* diffraction symmetry but assumed to be ordered (71.3% Au, 27.1% Cu, 1.6% Ag), and phase 3: the mineral tetra-auricupride (AuCu), with the ordered *P*4/*mmm* tetragonal structure (52.5% Au, 47.4% Cu, 0.1% Ag). The gold–copper alloys (phases 1, 2, 3) all correspond to phases that have been characterized in the synthetic Au–Cu system, although they rarely occur in nature. This study offers new information on natural Au_3Cu, which has been poorly characterized previously.

Keywords: Au–Cu alloys, tetra-auricupride, Au_3Cu compound, chemical composition, X-ray data, X-ray photoelectron spectroscopy, Kerr mine, Ontario.

SOMMAIRE

Le minerai à haure teneur dénommé "carbonate vert" de la mine Kerr (autrefois Kerr–Addison), près de Virginia, en Ontario, contient des grains d'or montrant différents degrés de remplacement par du cuivre lors d'un stade épithermal tardif. En lumière réfléchie, les alliages d'or et cuivre apparaissent en grains jaune-rosé, avec une réflectance légèrement plus basse que l'or pur, mais un meilleur poli. Ces alliages Au–Cu forment la bordure de grains d'or préexistants, dont le remplacement est favorisé au niveau des veinules les plus fines. L'or et trois alliages Au–Cu ont été reconnus, et caractérisés par analyse à la microsonde, diffraction X et spectroscopie photoélectronique X: phase 1: or avec Ag, Hg et Cu mineurs, structure désordonnée *Fm*3*m* (en pourcentages atomiques, Au 92.6, Ag 6.4, Hg 0.6, Cu 0.4); phase 1b: or avec teneurs prononcées mais variables en Ag et Cu (Au 89.9, Ag 7.3, Hg 0.4, Cu 2.4%); phase 2: alliage Au_3Cu, avec symétrie (par diffraction X) *Fm*3*m*, mais supposé ordonné (Au 71.3, Cu 27.1, Ag 1.6%); phase 3: tétra-auricupride (AuCu), de structure ordonnée quadratique *P*4/*mmm* (Au 52.5, Cu 47.4, Ag 0.1%). Les alliages or–cuivre (phases 1, 2 et 3) correspondent tous à des phases définies expérimentalement dans le système Au–Cu, bien qu'elles soient rares dans la nature. Cette étude apporte de nouvelles données améliorant la caractérisation de la phase Au_3Cu dans la nature.

(Traduit par la Rédaction)

Mots-clés: alliages or–cuivre, tétra-auricupride, composé Au_3Cu, composition chimique, diffraction X, spectroscopie photoélectronique X, mine Kerr, Ontario.

---

[1] To whom correspondence should be addressed. *E-mail address*: mfleet@julian.uwo.ca

INTRODUCTION

The synthetic Au–Cu system has been thoroughly investigated (*e.g.*, Okamoto *et al.* 1987), in light of uses of Au–Cu alloys in jewellery, medicine and dentistry, electrical and electronic devices in general, and numerous other industrial, technological and scientific applications. Gold–copper alloy compositions were among the earliest to have been subjected to analytical study, particularly with respect to their electrical and thermal conductivity (Matthiessen 1860, Heycock & Neville 1897), and order–disorder phase transformations (Kirchner 1922, Bain 1923). As described by Okamoto *et al.* (1987), six Au–Cu phases have been recognized and characterized: (Au,Cu) (*Fm*3*m*, A1 structure-type, continuous solid-solution), Au_3Cu (*Pm*3*m*, the $L1_2$ structure-type), AuCu I (*P*4/*mmm*, the prototype $L1_0$ structure), AuCu II (*Imma*), $AuCu_3$ I (*Pm*3*m*, $L1_2$ structure-type), and $AuCu_3$ II (*P*4*mm*). A modified phase-diagram for this system is shown in Figure 1.

Despite the abundance of theoretical and experimental work on Au–Cu alloys, very few examples of cupriferous gold have been found to occur in nature. This study reports one such occurrence of natural gold–copper alloys. This research was instigated at the request of mine staff at the Kerr mine for explanation of the red coloration of native gold in their ore, which was found to be attributable to a selvage of gold–copper alloys to the gold grains.

PREVIOUS WORK ON GOLD–COPPER ALLOY MINERALS

Data on the composition of synthetic alloys and other known references to gold–copper alloys are given in Table 1.

Ramdohr (1950, 1967, 1969, 1980) commented on auricupride ($AuCu_3$) and AuCu, mentioning an occurrence at the Kerr–Addison mine, as well as occurrences in "Rheingold" from Steinmauern, Baden, Germany, the

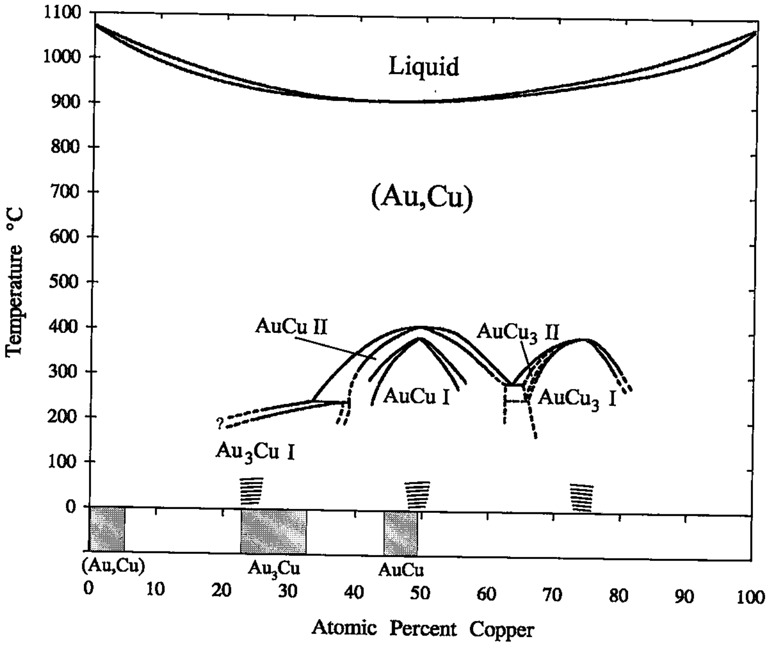

FIG. 1. Schematic phase-diagram for the system Au–Cu (after Okamoto *et al.* 1987), with suggested fields of stability at very low temperatures. The more restricted fields of the alloy phases stable at very low temperatures or in the presence of fluid are shown by hatching. The stability field of Au_3Cu II is not indicated. The composition of Au–Cu alloy phases from the Kerr deposit (identified by EMPA) are shown along the bottom axis.

TABLE 1. EMPA DATA ON REPORTED COPPER-GOLD MINERAL OCCURRENCES

Reference	Locality	Atomic % Composition		
		Au	Cu	Ag
Okamoto et al. (1987)	Synthetic alloys			
Au_3Cu	ideal (measured limit)	75 (85→61.5)	25 (15→38.5)	-
AuCu		50 (61.5→37)	50 (38.5→63)	-
$AuCu_3$		25 (37→17)	75 (63→83)	-
Chen et al. (1982)	Saar-Dala, China			
AuCu		50.5	49.5	-
Novgorodova (1983)	Karabash, Urals			
Au_4Cu		79.7	20.0	0.3
AuCu		45.4 (1.2)	54.0 (1.2)	0.6 (0.1)
$AuCu_3$		28.3 (1.7)	71.7 (1.2)	-
Novgorodova et al. (1977)				
AuCu		46.3 (2.3)	53.1 (2.3)	0.6 (0.2)
$AuCu_3$		28.3 (1.7)	71.7 (1.7)	-
Razin et al. (1971)	Talnakh, Siberia			
AuCu		50.1	49.9	-
Au_2Cu_3		40.0	60.0	-
Oen & Kieft (1974)	Beni-Bousera, Morocco			
$Au_{2.6}Cu$		72.2	27.8	-
Verryn et al. (1991)	Waaikraal deposit, S. Africa			
Au_3Cu		74.9	24.8	0.3
Stumpfl & Clark (1965)	Riam Kanan, Borneo			
Au_3Cu		71.2 (1.3)	27.5 (1.1)	1.3 (0.1)
AuCu		52.4 (2.1)	47.6 (2.1)	-
Au_2Cu_3		42.7	56.3	0.6
Ramdohr (1980)	Unknown source			
$AuCu_3$		17.7	82.3	-

Mooihoek platinum pipe, South Africa, at the Laxia to Mavrou deposit, Cyprus (Antun *et al.* 1966, Ramdohr 1967), and in unspecified localities in Victoria, Australia (Ramdohr 1950), and Tankavaara, Finland. Ramdohr described auricupride as "Red Gold" which, in polished section, exhibits a distinct lilac color, is harder than pure gold, and takes a better polish. However, the natural examples were considered to have nonideal compositions (40 wt.% Au, compared to the ideal value of 50.8 wt.% for $AuCu_3$; Ramdohr 1980). Paragenetically, Ramdohr (1967, 1969) considered auricupride to form in hydrothermal veins, typically in association with serpentinites, and within the experimentally determined field of stability of $AuCu_3$ at temperatures below 390°C.

An electron-microprobe (EMPA) investigation of argentian and cupriferous gold in alluvial concentrates from the Riam Kanan River, southeastern Borneo (Stumpfl & Clark 1965) showed considerable variation in gold contents among points analyzed (42.7 to 92.9 at.% Au). Among the mixed Au–Ag–Cu ore were grains of electrum, argentian gold and discrete phases rich in Cu, which gave microprobe data reflecting the stoichiometries AuCu, and Au_2Cu_3 to Au_3Cu. These analytical results were complicated by the variable Ag contents, up to 10.7 at.% in the Cu–Au alloys, and by the fine scale of intergrowth of the Au–Cu–Ag alloy within a Pt–Fe alloy.

Initial recognition and description of gold–copper grains from Karabash, southern Urals (Lozhechkin 1939) were continued by Novgorodova & Tsepin (1976) and also are summarized in Novgorodova *et al.* (1977) and Novgorodova (1983). On the basis of EMPA results, the cupriferous gold was found to comprise grains of AuCu with a Cu-rich border of auricupride ($AuCu_3$). They also reported rare compositions corresponding to $AuCu_4$ and a gold–silver amalgam ($Au_5Ag_{10}Hg$). A second occurrence of cupriferous gold from Russia, from the Talnakh Cu–Ni–PGE magmatic sulfide ores, was described by Razin *et al.* (1971), who reported a phase of stoichiometry Au_2Cu_3. Although they provided supporting X-ray-diffraction (XRD) data, Au_2Cu_3 is not a stable phase in the synthetic system (Okamoto *et al.* 1987). The phase Au_2Cu_3 has previously been termed "rozhkovite" (Razin *et al.* 1971) and "cuproauride" by Lozhechkin (1939), but these names have subsequently been discredited because the material actually comprised intergrown AuCu and auricupride.

Oen & Kieft (1974) reported several grains with a composition of $Au_{2.6}Cu$, from the Beni-Bousera Ni–Cr–Co–Au ores of Morocco. They noted that these grains have optical properties similar to those of native copper, and a composition of 72.2 at.% Au (88.35 wt.% Au). Oen & Kieft equated this mineral to the synthetic Au_3Cu phase, but did not provide supporting XRD data because of the fine grain-size and scarcity of the mineral. Another occurrence of the phase Au_3Cu was reported by Verryn *et al.* (1991) from a single grain in gold-bearing pyroxenites of the Waaikraal deposit, of the Bushveld Complex, South Africa.

More recently, Chen *et al.* (1982, 1983) reported a natural gold–copper alloy from the Saar-Dala mafic–ultramafic rocks along the upper Qingshui River, Malas County, Xingjiang Province, China. These authors reported a composition of 50.5 at.% Au (75.18 wt.% Au), 49.5 at.% Cu (23.74 wt.% Cu), and XRD analyses indicating the space group *P4/mmm* (*a* 2.815, *c* 3.720 Å), showing that the natural alloy is equivalent to the synthetic alloy phase AuCu I (Fig. 1), and establishing it as the mineral tetra-auricupride. In the Saar-Dala occurrence, tetra-auricupride is found within serpentinized pyroxenite, associated with PGE mineralization, along with native Au, Ag, magnetite, chromite, pyrrhotite, pyrite and chalcopyrite.

Ramdohr's (1969, 1980) references to the gold–copper alloys from the Kerr–Addison mine were not accompanied by a detailed description. Curiously, no mention of gold–copper alloys has been made in subsequent descriptions of the gold ore from the Kerr mine (Downes 1980, Kishida & Kerrich 1987, Smith *et al.* 1990). This study was instigated at the request of mine staff at the Kerr mine, who sought an explanation of the red coloration of the native gold in their ore. The red color, of course, is attributable to a selvage of gold–copper alloys to the gold grains. We here report the presence of cuprian gold, tetra-auricupride and another natural occurrence of the phase Au_3Cu in Kerr mine ore.

GEOLOGY AND GEOCHEMISTRY OF THE KERR MINE

The Kerr mine, formerly known as the Kerr–Addison mine, is located at Virginiatown, in the Kirkland Lake gold mining district of Ontario. The gold deposit is situated immediately south of the Kirkland Lake – Larder Lake fault zone, within mixed ultramafic–mafic extrusive volcanic rocks and their volcaniclastic sedimentary counterparts, all of Archean age (Warnick 1981, Kerrich 1983, Kishida & Kerrich 1987, Smith *et al.* 1990, 1993). As described in detail in Smith *et al.* (1993), the principal types of ore are characterized as "green carbonate – siliceous break" ores and "flow" ores. The host rocks of green carbonate ore are deformed komatiitic flows (Kishida & Kerrich 1987) with discontinuous spinifex horizons (Tihor & Crocket 1977). The bulk of the gold mineralization occurs as native Au deposited in composite, milky quartz-carbonate, "siliceous break"-related veins and quartz stringers. Potassic green carbonate alteration produced dispersed chromian mica as a selvage to Au-bearing veins. Essentially all gold values occur in the quartz veins and stringers; the green carbonate alteration itself does not host significant mineralization, and has low Au values. The average Au:Ag value (weight ratio) is approximately 18.2:1 in both green carbonate and flow ores (James *et al.* 1961, Warnick 1981), although Smith *et al.* (1991) described a smooth upward increase in Au:Ag ratio, from ~16:1 to ~21:1 at the 300 foot level (with Au approximately 94.1 to 95.5 wt.%). Main-stage ore minerals reported in green carbonate ore are gold, and minor pyrite, chalcopyrite, galena, sphalerite, enargite, scheelite, millerite, tetrahedrite, and traces of arsenopyrite (Warnick 1981, Smith *et al.* 1990). Channer & Spooner (1991) reported preliminary fluid-inclusion microthermometric data for ore from the 4014 foot level of the Kerr deposit. All trapped fluids are of the type $H_2O–CO_2–NaCl$. Homogenization temperatures of primary fluid-inclusions range from 220 to 320°C, and homogenization temperatures of inclusions in healed fractures range down to 135°C. Fluid-inclusion results, and vertical trends in wallrock alteration and gold grades, indicate that gold deposition was a result of $H_2O–CO_2$ phase separation.

At the Hollinger–McIntyre deposit, Timmins, Ontario, which was studied in more detail by Channer & Spooner (1991), temperatures of homogenization of aqueous secondary inclusions range down to below 100°C.

SAMPLES AND EXPERIMENTAL METHODS

Two pieces of green carbonate ore from the 300 foot level, 309 stope area of the Kerr mine, collected by mine staff in 1995, are the subject of this study. Gold grains were separated from the ore by simple mechanical crushing or by digestion of the gangue in hydrofluoric acid, followed by hand picking. The gold ore was studied by reflected-light microscopy, analytical scanning electron microscopy (SEM/EDX), EMPA, XRD, and X-ray photoelectron spectroscopy (XPS).

Electron-microprobe analyses were undertaken on a JEOL 8600 Superprobe, with an operating voltage of 20 kV and a current of 25 nA maintained on a Faraday

TABLE 2. COMPOSITION OF GOLD–COPPER ALLOYS FOUND AT THE KERR MINE (ELECTRON-MICROPROBE DATA)

Element	Phase 1 (primary gold)	Phase 1b (cuprian gold)	Phase 2 (Au_3Cu)	Phase 3 (tetra-auricupride)
		wt.%		
Au	95.5 (0.7)	94.5 (1.3)	87.6 (1.4)	76.6 (1.0)
Cu	0.1 (0.1)	0.8 (0.6)	10.8 (1.0)	22.3 (1.0)
Ag	3.6 (0.1)	4.2 (0.9)	1.1 (0.3)	0.1 (0.1)
Hg	0.6 (0.1)	0.5 (0.1)	0.0	0.0
Total	99.8	100.0	99.5	99.0
n =	14	15	22	8
		at.%		
Au	92.6 (0.3)	89.9 (2.8)	71.3 (2.0)	52.5 (1.4)
Cu	0.4 (0.3)	2.4 (1.8)	27.1 (2.1)	47.4 (1.4)
Ag	6.4 (0.1)	7.3 (1.5)	1.6 (0.4)	0.1 (0.1)
Hg	0.6 (0.1)	0.4 (0.1)	0.0	0.0

cup. Counts were collected for 20 (Au and Ag) or 30 seconds (Cu and Hg). Standardization was based on pure Au, Ag, and Cu, and HgS. The rare grains of sulfide present in the samples were standardized against millerite, pyrite, pure cobalt, arsenopyrite, and stibnite, with counts collected 20 seconds per element (Ni, Fe, Co, As, Sb, S). EMPA results for the gold–copper alloys are given in Table 2.

The X-ray-diffraction investigation included powder XRD (P–XRD) using Gandolfi and Debye–Scherrer cameras (Cr$K\alpha$ X-radiation, λ = 2.2909 Å), a study by X-ray precession of polycrystalline flakes of gold, and P–XRD of polycrystalline flakes mounted in Vaseline, using a Rigaku high-brilliance rotating anode XRD (Co$K\alpha$, λ = 1.79021 Å). More than 12 individual polycrystalline flakes of gold, representing a range of size and colors (from yellow to red), were examined by Gandolfi P–XRD, and several aggregates of polycrystalline flakes were examined by Debye–Scherrer P–XRD. A representative powder pattern is reported in Table 3, and unit-cell parameters, in Table 4.

X-ray photoelectron spectroscopy analysis was performed on a modified Surface Science Laboratories SSX–100, with a monochromatized Al$K\alpha$ X-ray source. The spectrometer work function was adjusted to give a value of 84.0 eV for the Au $4f_{7/2}$ peak of metallic gold, and spectra were also calibrated to the C 1*s* peak at 285 eV. Further details of instrument settings and XPS peak-fitting parameters may be found in Mycroft *et al.* (1995).

RESULTS

Ore microscopy

Gersdorffite and millerite are the only two sulfide minerals identified in the thin sections studied, occurring in association with one another and with the primary gold mineralization. Gersdorffite is dominant over millerite; it forms coarse, occasionally subhedral grains, which exhibit partial atoll formation. Millerite occurs marginal to, or as inclusions within, gersdorffite. In reflected-light microscopy, it exhibits a slightly anomalous green-grey color (due to minor cobalt), weak reflection-pleochroism, anisotropic colors from dark brown to blue-grey, and takes a better polish than the surrounding gersdorffite.

Primary gold is localized along grain boundaries in quartz, forming thin stringer and coarse anhedral grains, up to 300 × 50 μm in size. Polycrystalline gold is adjacent to and intergrown with sulfides, although the presence of gold filling brittle fractures in gersdorffite suggests that precious-metal mineralization post-dated sulfide mineralization.

The gold–copper phases are present as discontinuous pink-yellow zones at the margins of the larger primary polycrystalline grains of gold, at grain boundaries with gangue minerals, and as a more pervasive replacement of thin stringer gold grains plating quartz grains (Fig. 2). The pink gold took a better polish than yellow gold and has a slightly lower reflectance. Under crossed nicols, the gold–copper alloys are isotropic and appear brownish; they do not display the anomalous green internal reflections characteristic of pure gold.

Grains of the gold–copper alloys (identified by microprobe as Au_3Cu and AuCu, and discussed below) are too intimately intergrown and have too similar optical properties to be resolved in reflected-light microscopy. Similarly, reflectance data for the individual gold–copper alloys could not be obtained owing to their fine grain-size. Reflectance data for tetra-auricupride (AuCu; phase 3 of this study) are, however, reported in Chen *et al.* (1982, 1983). Similarly, we were not able to resolve areas of cuprian gold, which had been identified by electron-microprobe analysis (Table 2), from primary gold by reflected-light microscopy.

A single occurrence of small (<2 μm), bladed inclusions of a purple-grey, moderate-reflectance mineral was found within a Au–Cu grain surrounded by grains of gersdorffite. These unidentified grains exhibit instability to light, and disappeared before electron-microprobe analysis could be undertaken. The photosensitivity, optical properties and location within the Au–Cu grain suggest that the unknown mineral either belonged to the Cu–Ag–S group of minerals (*e.g.*, stromeyerite [CuAgS]; jalpaite [Ag_3CuS_2]; mckinstryite [$(Ag,Cu)_2S$]), or was a sulfosalt of silver.

The gangue minerals in the samples studied consist of quartz, green chromian mica ("fuchsite") and carbonates, and were not studied in detail.

Electron-microprobe analysis

Four compositionally distinct regions in the grains of gold were readily distinguished by back-scattered electron (BSE) imaging, with the Cu-rich areas appearing

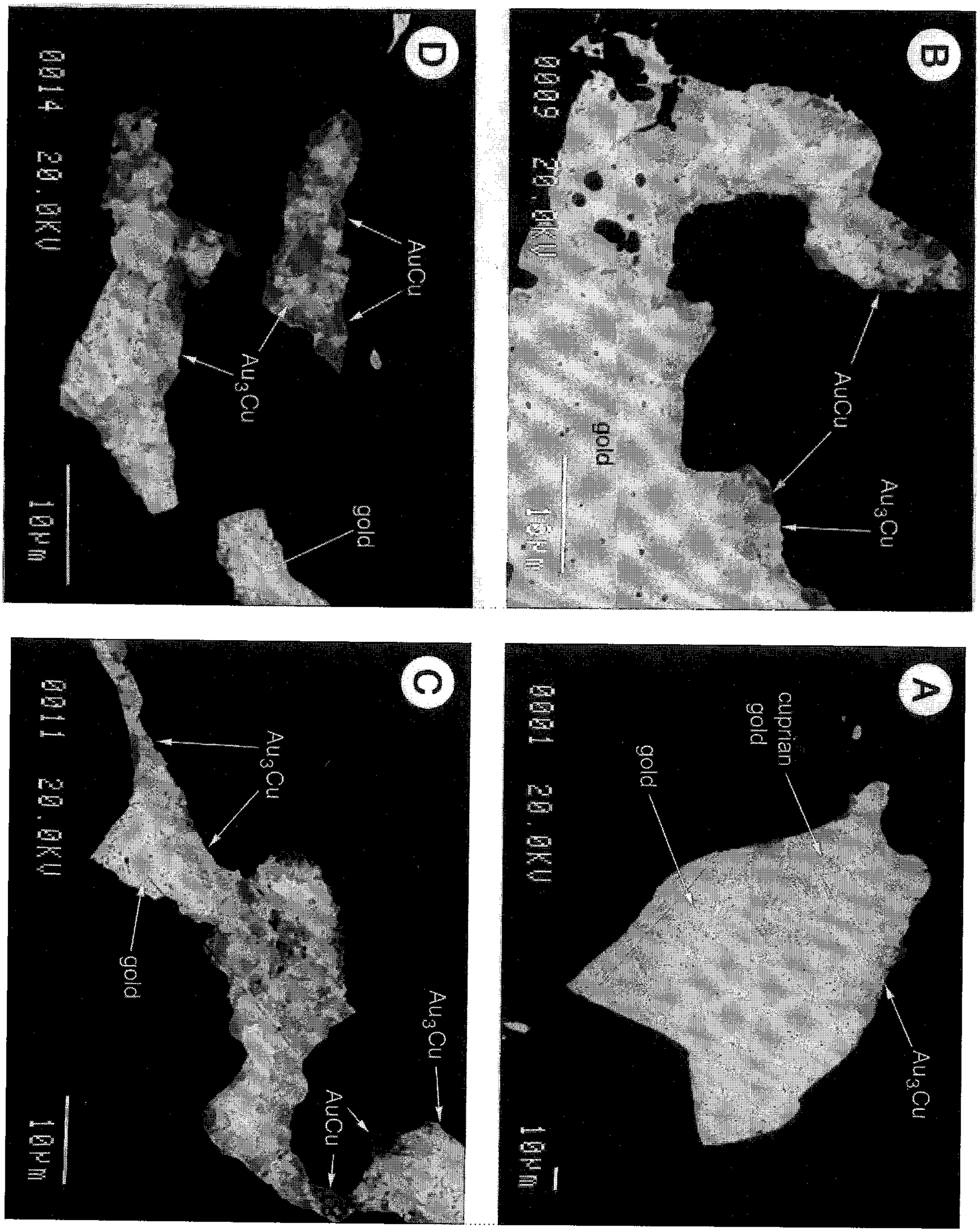

FIG. 2. (A) Back-scattered electron (BSE) micrograph of gold grain comprising primary gold (phase 1), cuprian gold (phase 1b), and Au_3Cu (phase 2). Phase 2 forms where phase 1b meets the grain margin in contact with gangue. (B) BSE micrograph, showing marginal replacement of primary gold (phase 1) by Au_3Cu (phase 2) and minor tetra-auricupride (AuCu; phase 3). (C) BSE micrograph of more pervasive Cu alteration, localized in grains of stringer gold interstitial to grains of quartz, showing fine intergrowth of gold and alloy phases 1, 2, and 3. (D) BSE micrograph illustrating complete replacement of a small grain of primary stringer gold by phases 2 and 3.

as dark contrast (Fig. 2). We have labeled these visually and compositionally distinct regions: phase 1 (gold), phase 1b (cuprian gold), phase 2 (Au_3Cu), and phase 3 (AuCu; tetra-auricupride). The gold–copper phases (1b, 2, 3) are associated only with grains of "red" gold.

The average composition of primary yellow gold (phase 1) is given in Table 2; the recorded range in gold compositions is 91.9–92.9 at.% Au, 6.3–6.5% Ag, 0.4–0.7% Hg and 0.2–1.2% Cu. With a Au:Ag ratio of ~26.5:1 (by weight), this is slightly less strongly argentian than the average composition of gold from the Kerr mine (~18.2:1; Warnick 1981), although the recorded value of 95.5 wt.% Au (Table 2) conforms closely to the Au:Ag ratio from upper levels at the Kerr mine (Smith *et al.* 1991). Therefore, we assume that phase-1 gold represents a primary composition. Certainly, the gold–copper mineralization event that led to phases 2 and 3 is marked by a depletion in Ag.

Cuprian gold (phase 1b) occurs sporadically, as a pervasive replacement of primary gold grains (*e.g.*, Fig. 2a). It is occasionally associated with the marginal replacement by phases 2 and 3, but also seems to occur alone. The average composition of phase 1b gold is given in Table 2; however, the significant range in recorded compositions (84.6–92.9 at.% Au, 6.3–10.6% Ag, 0.3–5.1% Cu, 0.2–0.6% Hg) reflects a mottled, bimodal distribution of alloy compositions, with Cu-rich and Ag-enriched patches intimately mixed within a matrix of primary gold.

Phases 2 and 3 (Au_3Cu, and AuCu, tetra-auricupride) occur together as a marginal replacement of larger primary grains of gold (Fig. 2b), (phase 1) and more rarely of phase 1b (Fig. 2a), and as a pervasive replacement of grains of stringer gold (Figs. 2c, d). For phases 2 and 3, the replaced areas of the grains of primary gold correspond to the areas of pink-yellow coloration in reflected light. Individual grains are up to 10 µm in longest dimension, with phase 2 tending to form the larger, volumetrically greater, and more homogeneous grains. Grains of these two Cu-rich alloy phases are not homogeneously distributed, *i.e.*, phase 3 is generally more abundant toward the margin of gold grains. Thus there is a well-defined paragenetic relationship of primary gold (± phase 1b), followed by phase 2 and, finally, phase 3.

Analyses of phase 2 gave a compositional range 65.6–75.0 at.% Au, 23.6–33.3% Cu, 1.3–3.0% Ag, with an average composition that corresponds to Au_3Cu (Table 2). We equate this phase to the synthetic alloy phase Au_3Cu (Fig. 1; Okamoto *et al.* 1987). Analyses of phase 3 gave a compositional range 50.8–54.9 at.% Au, 44.8–49.1% Cu, 0.1–0.% Ag. The average composition of phase 3 (Table 2) corresponds to the formula AuCu, which is clearly the mineral tetra-auricupride (Chen *et al.* 1982, 1983). As for associated sulfide minerals, EMPA analysis of gersdorffite [NiAsS] and millerite [NiS] gave virtually ideal compositions, with trace Sb, Co and Fe in gersdorffite, and minor Co in millerite. Neither mineral contains detectable amounts of copper.

TABLE 3. POWDER-DIFFRACTION PATTERNS§ OF GOLD–COPPER ALLOYS FOUND AT THE KERR MINE

Composite Pattern					1, Au gold		2, Au_3Cu		3, AuCu tetra-auricupride	
line	2θ(°)	d (Å)	I/I_0	Assignment	*hkl*	d(calc)	*hkl*	d(calc)	*hkl*	d(calc)
1	36.68	3.6403	3.5	3					001	3.6712
2	48.42	2.7932	2.0	3					100	2.8062
3	58.67	2.3381	20	1	111	2.3503				
4	60.17	2.2850	13	2			111	2.2974		
5	62.02	2.2234	15	3					101	2.2295
6	68.81	2.0272	14	1	200	2.0355				
7	70.51	1.9844	13	2,3			200	1.9896	110	1.9843
8	73.76	1.9086	0.1							
9	77.21	1.8358	1.5	3					002	1.8356
10	80.31	1.7763	0.3							
11	82.05	1.7451	1.0	3					111	1.7456
12	96.35	1.5371	1.5	3					102	1.5362
13	101.82	1.4758	0.2							
14	105.79	1.4362	25	1	220	1.4393				
15	109.24	1.4049	15	2,3			220	1.4069	200	1.4031
16	116.39	1.3478	13	3, 1*	311				112	1.3475
17	122.03	1.3095	1.0	3					201	1.3106
18	131.73	1.2552	1.5	3					120	1.2550
19	137.87	1.2275	100	1	311	1.2274				
20	145.52	1.1993	20	2			311	1.1998		
21	149.47	1.1873	15	3					211	1.1875
22	154.26	1.1750	35	1	222	1.1752				

§ Cr*K*α radiation, λ = 2.2909 Å. Assignments: phase 1 is gold [*a* 4.0709(12) Å], phase 2 is Au_3Cu [*a* 3.9792(29) Å], and phase 3 is tetra-auricupride, AuCu [*a* 2.8062(17), *c* 3.6712(23) Å]. * marks overlap with 311 (*K*β) of gold.

TABLE 4. PROPERTIES OF GOLD MINERALS IN RED GOLD ORE FROM THE KERR MINE, ONTARIO

phase	1	2	3
mineral/phase	gold	Au_3Cu	tetra-auricupride
occurrence	quartz vein; quartz grain boundaries	marginal replacement of 1	marginal replacement of 2
space group	Fm3m	(Pm3m)[1]	P4/mmm
a (Å)	4.071(1) [TSNR][2]	3.979(3) [TSNR]	
a (Å)	4.068(3) [LS][3]	3.975(3) [LS]	2.806(2) [LS]
c (Å)			3.671(2) [LS]
cell volume ($Å^3$)	67.46	63.01	28.91
density (D_x: $g.cm^{-3}$)	18.78	16.80	15.35
Cu (at.%): EMPA	0.4	27.1	47.4
Cu (at.%): P-XRD[4]	3	27	52

1. apparent P-XRD diffraction summetry is Fm3m; 2. TSNR is by extrapolation to 180° (2θ) (cf. Azaroff and Buerger, 1958); 3. LS is least-squares refinement with equal weight to all lines; 4. using cell-edge *vs.* binary Au-Cu composition calibration of Okamoto et al. (1987).

X-ray-diffraction analysis

X-ray powder diffraction with Gandolfi and Debye–Scherrer cameras yielded composite powder patterns of the three phases, 1, 2, and 3. A composite powder pattern is reproduced in Table 3. No diffraction lines were ascribed to phase 1b.

Line assignments and identification were based on Powder Diffraction System file 4–0784 for gold (phase 1), Kubiak & Janczak (1991) for Au_3Cu (phase 2), and Johannson & Linde (1936), Novgorodova *et al.* (1977) and Chen *et al.* (1982, 1983) for tetra-auricupride (AuCu, phase 3).

Important powder-diffraction lines of Au_3Cu and tetra-auricupride overlap (*e.g.*, 200 and 110, 220 and 200, respectively; Table 3). However, the three phases are readily distinguished by separation of 111 and equivalent 111 lines (*e.g.*, Fig. 3). The proportion of the three phases present varies markedly from sample to sample (of polycrystalline grains). Patterns of larger grains are dominated by lines of primary gold, whereas thin red flakes of stringer gold (*e.g.*, Figs. 2c, d) yield patterns with tetra-auricupride lines dominant.

Strong absorption suppress the intensities of low-2θ lines and introduce systematic error in the determination of unit-cell parameters. Therefore, the preferred values of the cell edge of gold and of Au_3Cu (Table 4) are those obtained by Taylor-Sinclair-Nelson-Riley extrapolation to 2θ=180° (*e.g.*, Azaroff & Buerger 1958).

Au_3Cu is characterized by lines of the face-centered cubic structure only (*Fm*3*m* diffraction symmetry). Powder lines (or side bands) characteristic of the $L1_2$ structure-type (primitive lattice) were not evident. Tetra-auricupride is characterized by lines of the ordered tetragonal structure (space group *P*4/*mmm*) (synthetic alloy phase AuCu I). Side-bands indicative of AuCu II (*e.g.*, Barrett & Massalski 1966) are not present.

Precession photographs revealed reflection spots of polycrystalline gold (phase 1), broadened into incomplete powder rings, and faint powder rings of phase 2. Evidently, the gold–copper alloy phases Au_3Cu and tetra-auricupride are not in crystallographic continuity with crystals that make up the gold substrate; *i.e.*, the replacement was not topotactic.

X-ray photoelectron spectroscopy

XPS was used to investigate possible effects on element binding energies, as a function of electron-charge equilibration due to alloying. Previous studies on gold–copper alloys (Castellani & Leroy 1988, Yoshitake & Yoshihara 1991, Jordan *et al.* 1991) indicated a shift in binding energy of approximately +0.3 eV for the Au $4f_{7/2}$ peak, and –0.26 eV for Cu $2p_{3/2}$, in samples of Au_{100} to $Au_{50}Cu_{50}$ composition.

The present results are preliminary and were obtained from a sample of three flakes of gold that have a red tint. Broadscan XPS spectra, acquired with a 600-μm spot size, gave Au:Cu ratios of 75:25 to 85:15; note, however, that both gold and copper signals are weak owing to large amounts of surface oxygen and carbon.

Narrow-region spectra of the Au 4*f* and Cu $2p_{3/2}$ peaks, acquired with a 300-μm spot size, were used to investigate potential shifts in binding energy. The Au 4*f* spectra of the "red" gold produced narrow peaks, comparable in shape and intensity to the pure gold calibration standard; however, the binding energy is shifted by +0.45 eV relative to the standard, consistent with gold alloyed with copper.

The Cu $2p_{3/2}$ spectrum is composed of a signal from three species, at (i) 932.4 eV, (ii) 933.46 eV and (iii) 935.7 eV. "Shake-up" peaks (Briggs & Seah 1985) are present at approximately 10 eV higher, indicative of CuO, which has recorded binding energies of 933.5–934 eV (Moulder *et al.* 1992). Species (iii), with the highest recorded binding energy, was attributed to CuO. Changes in electrical charge with alloying should result in a decrease in binding energy from native Cu (cited at 932.5–932.8 eV). Both species (i) and (ii) are attributed to Cu in Cu–Au alloys, of two distinct compositions. Given the inferior spatial resolution and surface sensitivity (approximately 10 Å depth) of XPS, we were not able to further correlate these results with the alloy phases recognized by EMPA. Since the XPS analyses were made on the surfaces of chemically separated flakes, we anticipated significant contributions from phases 2 and 3. Also, the CuO clearly represents a tarnish film, which could have formed during sample preparation. The recorded Au:Cu ratio from broadscan analysis probably represents a mixture of surface gold–copper species, although there is probably a significant degree of error in the Au:Cu values.

DISCUSSION

Gold–copper alloy minerals at the Kerr mine

The physical and crystallographic properties of the Au–Cu phases from the Kerr mine are summarized in Table 4. Both EMPA and XRD indicate that the main Au–Cu phases (1, 2, 3) have discrete compositions and crystallographic structures, which all correspond to phases established in the synthetic Au–Cu alloy system. Reflectance measurements were futile owing to the fine scale of the intergrowth between phases 2 and 3, which could not be differentiated by optical microscopy, even after areas had been characterized by EMPA.

The physical properties of the Au–Cu mineralization, *i.e.*, pink coloration, slightly lowered reflectance, increased hardness and improved polish, are consistent with those described from other occurrences (Ramdohr 1980), and are consistent with the features expected from Au–Cu alloys.

Phase 1 is consistent with gold containing minor silver, copper and mercury (Ramdohr 1969, 1980), found in many ore deposits. This gold has the face-centered cubic (*Fm*3*m*) structure, consistent with the Au–Ag–(Cu) solid solution. The measured *a* cell parameter, 4.071(1) Å, shows a minor deviation from an ideal value, 4.0784 Å, for pure gold (Okamoto *et al.* 1987). This difference is attributed to the substitution of Ag, and minor Cu and Hg, for Au.

Phase 1b exhibits a higher degree of variability in composition than the other alloy phases. The composition shows an increase in Ag and Cu compared with phase 1. The average difference in composition between phases 1 and 1b is Cu +2.0 at.% and Ag +0.9 at.%, although the maximum recorded EMPA contents of Cu and Ag show significant local enrichment (5.1 at.% and 10.6 at.%, respectively). Electron-microprobe results also show that phase 1b is not homogeneous, with compositions of local areas being virtually identical to that of phase 1. This implies that even within darker regions on BSE images, there exist areas at least 1 μm in diameter that have a composition of primary unaltered gold (phase 1). It is conceivable that phase 1b is composed of small intergrown domains of phases 1 and 2. This could potentially be substantiated by transmission electron microscopy (TEM). The textural appearance of phase 1b, occurring as a pervasive alteration occasionally with sharp margins (along intragrain boundaries), is consistent with infiltration of fluid. Thus, phase 1b may represent the replacement front of the Cu-bearing fluid responsible for the Au–Cu mineralization.

The powder-diffraction lines for the phase 2 Au–Cu alloy are consistent with the face-centered cubic *Fm*3*m* structure. The unit-cell edge, 3.979(3) Å, corresponds to a copper content of 27 at.%, using the calibration of cell edge *versus* binary Au–Cu composition of Okamoto *et al.* (1987), which compares favorably with our EMPA composition (27.1 at.% Cu, 71.3% Au).

The diffraction pattern of phase-2 gold exhibits no lines that can be attributed to periodic antiphase structures (PAP) or long-range order (LRO) in general (*e.g.*, Batterman 1957, Okamoto *et al.* 1987). Okuzumi *et al.* (1959) and Toth & Sato (1963) also reported ordering at or near the Au_3Cu composition, giving the $L1_2$ structure (Au_3Cu I type) equivalent to that of $AuCu_3$. Such ordering was produced by annealing the alloys at moderate temperatures (*e.g.*, 150–170°C for 45–120 days; Lu & Liang 1966a, b). The low value of the transition temperatures for the Au_3Cu composition led to some misleading interpretations on the onset of ordering, but it is now well established by TEM studies that annealed Au_3Cu does exhibit both PAP (Au_3Cu II) and $L1_2$ (Au_3Cu I) structures (Gratias *et al.* 1972, Bessière *et al.* 1983). In fact, ordering at the Au_3Cu composition is spontaneous and rapid below the transition-temperature range, in spite of the very low temperatures involved. Au_3Cu quenched from immediately above the transition temperature invaribly exhibits short-range ordering (SRO; Batterman 1957, Bessière *et al.* 1983), even though the XRD symmetry is *Fm*3*m*. The critical temperature (T_c) for the order $\rightleftharpoons$ disorder transition of the Au_3Cu composition is 199 ± 3°C (Batterman 1957), as indicated by the disappearance on heating of the two low-2θ-angle reflections (100 and 110) that characterize the $L1_2$ structure-type. However, this temperature is probably an upper-bound value for T_c (*cf.* Gratias *et al.* 1972). More recently, Kubiak & Janczak (1991) annealed an initially disordered alloy of composition Au_3Cu at 270°C for 182 days. The product consisted of minor AuCu I in a cubic *Fm*3*m* matrix. They suggested that AuCu is the only stable ordered alloy phase in the Au–Cu system. However, this reasoning is flawed because their experiment was conducted above the transition temperature for ordering of the Au_3Cu composition. Their experimental results really only relate to the stability of AuCu and have no bearing on the stability of Au_3Cu and $AuCu_3$.

Analysis of the recorded powder-diffraction patterns for phase 3 reveal a tetragonal symmetry, with unit-cell parameters *a* 2.806(2), *c* 3.671(2) Å (Tables 3, 4). The *Fm*3*m*-equivalent (cubic) cell edge (*a* = 3.867 Å) corresponds to a copper content of 52 at.%, using the calibration of cell edge *versus* binary Au–Cu composition of Okamoto *et al.* (1987). This compares favorably with the mean EMPA composition, 47.4 at.% Cu, 52.5% Au for grains of phase 3. The composition and tetragonal unit-cell parameters for the phase-3 Au–Cu alloy closely correspond to tetra-auricupride (AuCu, Chen *et al.* 1982, 1983) and to the synthetic alloy AuCu I (Okamoto *et al.* 1987).

The absence of a continuous suite of Au–Cu compositions, and the correspondence to characterized synthetic phases (*i.e.*, AuCu I, Au_3Cu), suggest that the main gold alloy phases in this study (1, 2 and 3) are all discrete and can be considered as separate minerals. Whereas several examples of Au_3Cu (phase 2) have been identified by previous investigators (Table 1), this natural phase has not been defined as a mineral.

Although we have not investigated phase 2 by TEM, the laboratory studies on annealed Au_3Cu alloys (*e.g.*, Batterman 1957, Bessière *et al.* 1983) leave little doubt that this natural alloy at least possesses SRO, with its constituent atoms locally clustered in the manner of the $L1_2$ structure. For this reason, Table 4 shows phase 2 as having the space group *Pm*3*m*.

Because the atomic number of gold (79) is so much greater than that of copper (29), the relative intensities of equivalent XRD reflections change markedly across the binary Au–Cu join. The calculated relative P–XRD intensities of the 100 and 110 reflections (I_{100}/I_{111}, I_{110}/I_{111}) that characterize LRO in these face-centered cubic alloys increase progressively from Au_3Cu I (1×), to AuCu I (~2×) and $AuCu_3$ I (~3×). Moreover, for synthetic Au_3Cu alloys that are slightly off the stoichiometric composition, low-temperature annealing leads to very imperfect order, and superlattice spots may be so weak that it is impossible to observe the intergrowth morphology by TEM (Gratias *et al.* 1972). Thus, the low-2θ-angle reflections 100 and 110 are weak in P–XRD patterns of Au_3Cu I and are less likely to be resolved with the limited quantity of phase 2 available in this study (*cf.* Fig. 3). Although we were able to separate a flake of gold for P–XRD with phase 3 (AuCu, tetra-auricupride) dominant over phase 1 and

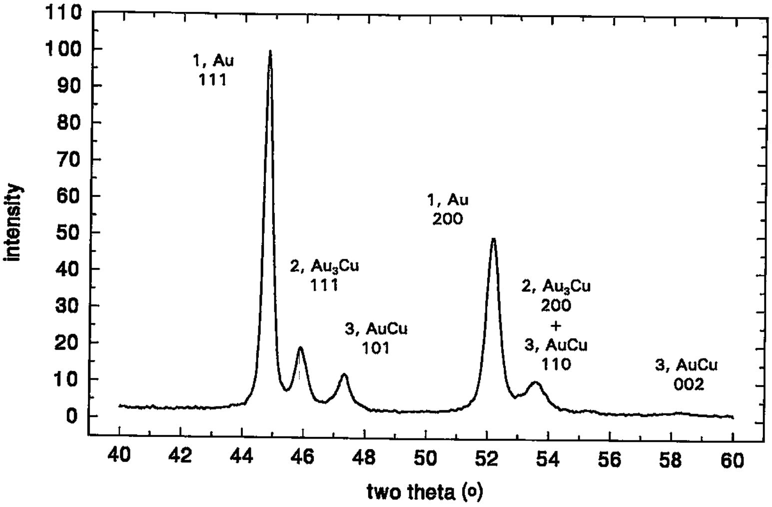

FIG. 3. Part of a powder-XRD diffractometer spectrum of polycrystalline flakes of "red" gold from the Kerr mine. Reflection assignments for primary gold (phase 1), Au_3Cu (phase 2), and tetra-auricupride (AuCu; phase 3) are shown. (Co*K*α, λ = 1.79021 Å).

phase 2, phase 2 does not occur as the dominant phase in any flake of gold investigated. Phase 2 is present only in subordinate amounts in all flakes examined by XRD despite EMPA studies indicating it is volumetrically more significant than phase 3. Therefore, the absence of evidence for both SRO (diffuse scattering intensity) and LRO (100, 110 reflections) is understandable. We assume that Au_3Cu from the Kerr mine has either the ordered $L1_2$ structure (*cf.* Au_3Cu I) or a local structure of domains of the $L1_2$ structure (*cf.* mixture of Au_3Cu I and Au_3Cu II). Although the ordered Au–Cu alloys exhibit broad ranges in solid solution under laboratory conditions, with maximum ranges that are indeterminate for Au_3Cu I, 37–62 at.% Au for AuCu I, and 20–33 at.% Au for $AuCu_3$ I, they appear to have restricted compositions in nature (this study, Chen *et al.* 1982, Ramdohr 1980). This no doubt is a reflection of the much longer annealing time and involvement of fluids in the natural environments.

Other natural occurrences of gold–copper alloys

Although the number of reported occurrences is small, natural Au–Cu alloys are invariably associated with ultramafic and mafic host-rocks that typically have undergone some degree of alteration (hydrothermal or weathering), and are commonly associated with PGM mineralization. These features are common to: (i) the tetra-auricupride occurrence in Saar-Dala, Qingshui River, Xingjiang Province, China, that is hosted in a serpentinized pyroxenite dyke, and associated with Pt mineralization (Chen *et al.* 1982); (ii) Au–Cu grains from the Karabash deposit of the Urals, Russia (Novgorodova & Tsepin 1976), that are associated with Paleozoic volcanic and sedimentary rocks overlying an ophiolite sequence, which is Pt-bearing at its western extremity (Khain 1985). In addition, other localities in the Urals are also known to contain native Cu, Cu–Zn and Au–Ag mineralization (Craig & Vaughan 1981); (iii) the Au–Cu occurrence at the Talnakh deposit, Russia (Razin *et al.* 1971), is hosted by mafic intrusive bodies and includes economic Ni–Co–PGM ore; (iv) Au–Cu grains recovered from the Mooihoek Pt pipe, South Africa (Ramdohr 1969, 1980), that is composed of ultramafic pegmatoids around a pyroxenite intrusive pipe; (v) grains of $Au_{2.6}Cu$ formed along grain boundaries of nickeline and löllingite, within Ni–Cr ore from the ultramafic rocks of Beni-Bousera, northern Morocco (Oen & Kieft 1974); (vi) AuCu and auricupride from the Laxia to Mavrou deposit in the Troodos ophiolite complex of Cyprus (Antun *et al.* 1966); (vii) alluvial concentrates of platinum-group minerals from southeast Borneo that contain Au–Cu grains derived from weathering of an ophiolite complex (Stumpfl & Clark 1965). In an ensuing discussion of this work (Stumpfl & Clark 1966), mention was made of gold–copper alloys from an undisclosed locality in northern Morocco [possibly the Beni-Bousera ophiolitic occurrence reported by Oen & Kieft (1974)]. In this same discussion, Stumpfl & Clark (1966) attributed a Cu-rich rim around Pt grains from the Nizhny Tagil PGE deposit of the Urals to partial replacement of Pt by migrant Cu released during serpentinization of host dunites.

The Kerr gold deposit occurrence appears to fall within this general petrological environment, having host rocks of deformed and carbonatized komatiitic flows, although there is no large-scale serpentinization within the deposit, and no PGE mineralization.

The gold–copper alloys from the Kerr mine correlate much more closely with phases from the synthetic alloy system than do the alloys from many of the other known natural occurrences. Ramdohr (1980) commented on the variability and lack of stoichiometry in the natural occurrences of AuCu and auricupride ($AuCu_3$), the latter with a cited composition of 17.7 at.% Au, as opposed to an ideal 25 at.% Au. Similarly, the suite of reported natural compositions prior to this study included $Au_{2.6}Cu$, Au_2Cu_3 and $AuCu_4$, in addition to AuCu and $AuCu_3$.

The descriptions of Au–Cu grains from the Karabash region, Russia (Novgorodova & Tsepin 1976), and from Saar-Dala, Xingjiang Province, China (Chen *et al.* 1982), are very similar to the grains of Au_3Cu and AuCu from the Kerr mine. In all of these localities, gold–copper alloys are located around the periphery of grains of unaltered primary gold, with an increase in copper content toward grain margins. The size of the tetra-auricupride grains from Saar-Dala (up to 600 μm; Chen *et al.* 1982) is very much larger than in the present study (1–5 μm). The presence of a AuCu core and a $AuCu_3$ rim in alloy grains from both Saar-Dala and Karabash indicates replacement of primary gold by either a larger volume of fluid or a more Cu-rich fluid than that responsible for formation of the Au–Cu alloys at the Kerr deposit. A greater volume of fluid would also result in the more complete alteration of large grains of primary gold, perhaps explaining the larger size of the Au–Cu alloy grains from the Saar-Dala and Karabash deposits.

Formation of gold–copper alloys at the Kerr mine

Despite similarities in host environment and style of mineralization of Au–Cu alloys, there has been little direct discussion on their mode of formation. Texturally, the localization of the copper mineralization at the margin of pre-existing grains of primary gold, and the increase in copper content at grain boundaries and within thin stringer gold, are consistent with Au–Cu alloy formation *via* the replacement of primary gold by Cu. This is logically attributed to a late-stage infusion of Cu-bearing fluid. Copper may have been concentrated in a residual fluid responsible for the gold mineralization, or may represent remobilization of copper from adjacent host-rocks (*cf.* Saar-Dala, China) or pre-existing concentrations of ore (*cf.* Karabash, Russia). The presence of hydrothermal or weathering-related alteration of host rocks in many of the previously documented occurrences of Au–Cu alloys (Ramdohr 1967) suggests that the copper was derived by remobilization. This also appears to be have been the case at the Kerr mine, where there are no copper sulfides nor copper-bearing sulfides associated with the primary gold mineralization. Thus the fluids responsible for primary gold mineralization probably contained little copper. Obviously, host ultramafic–mafic rocks are a good source for Cu, and this is likely reflected in the ubiquitous association of ultramafic–mafic rocks as hosts to all reported Au–Cu alloy occurrences.

Vein chronology and fluid-inclusion studies of the Kerr mine (Smith *et al.* 1990, Channer & Spooner 1991) indicate that the temperature of the main episode of gold mineralization decreased from ~340 to 280°C. However, these authors also reported the occurrence of healed quartz veins containing aqueous fluid inclusions of variable salinity, which postdated the main episode of gold mineralization; these inclusions have temperatures of homogenization of ~130°C. This very low temperature is in accordance with that dictated by the stability field of synthetic Au_3Cu, which lies below 240°C (Fig. 1; Okamoto *et al.* 1987).

There is also evidence of late reactivation along adjacent parts of the Larder Lake fault, resulting in *en échelon* extensional veinlets containing Au–Ag–Cu mineralization (Tourigny *et al.* 1993). However, no such veining or fault reactivation has been noticed at the Kerr deposit (Smith *et al.* 1993).

The formation of very-low-temperature copper-bearing fluids, akin to those probably responsible for natural Au–Cu alloys, has been studied in detail with respect to large stratiform sediment-hosted copper deposits, *e.g.*, White Pine and Keweenawan Peninsula, both in Michigan, Kupferschiefer, in northern Europe, Zambian Copper Belt, Zambia and Zaire, and other deposits (Brown 1974, Boyle *et al.* 1989). Copper is found to be soluble in a number of aqueous environments; *e.g.*, in acidic waters ($pH < 6.5$), in fluids with high concentrations of dissolved chloride, in fluids with high pCO_2, and organic-matter-rich fluids (Rose 1989). The conditions for solubility are similar at 100–200°C, although a higher pCO_2 is more likely at higher temperatures. Deposition of copper in stratiform sediment-hosted copper deposits is commonly reported to occur at a redox boundary, either as a result of fluid mixing (*e.g.*, Olympic Dam; Johnson & McCulloch 1995) at the interface between reduced mineralizing fluids and oxidized groundwaters, or at a stratigraphic interface, for example an organic-matter-rich sedimentary horizon (*e.g.*, Schwartz *et al.* 1995). The late-stage copper mineralization at the Kerr mine is localized only near grains of primary gold.

The presence of silver mineralization, associated with copper and in the absence of sulfides, has been inferred to constrain the nature of the mineralizing fluids; they must have been moderately to highly oxidized, with a basic pH (>7.5–9) (Rose 1989). The coeval enrichment in Ag and Cu associated with phase 1b gold in the present study is thus inferred to involve an oxidized fluid of relatively high pH. This fluid appears to have rapidly lost silver, but continued to replace gold by copper, successively forming phases 2 and 3. Alternatively, the local high Ag contents of cuprian gold from the Kerr mine may simply reflect primary Ag that was locally remobilized within the replaced grains of gold by the infiltration processes.

The shallow depth from which the present samples were recovered, roughly 100 m, make it a distinct possibility that the gold ore at the Kerr mine was accessible to oxidized groundwaters. However, the absence of extensive oxidation of either the gangue or other ore minerals adjacent to the gold (*i.e.*, absence of millerite and gersdorffite) suggests that the fluids responsible for the Au–Cu mineralization were not present-day groundwaters. Similarly, a study of vertical trends in the Kerr–Addison mineralizing system led Smith *et al.* (1991) to suggest that the Kerr deposit was not exposed to the Archean paleosurface.

Therefore, the fluids responsible for Au–Cu alloy mineralization were most likely those of the late-stage fluid inclusions in healed quartz grains, reported by Channer & Spooner (1991). These fluids were reported to have salinities consistent with a mixture of fluids (4–4.7 wt.% eq. NaCl), moderate CO_2, and formation temperatures of ~130°C. We suggest that the transporting fluids were relatively oxidized, fairly basic and of low sulfur fugacity. Copper could have been derived from adjacent ultramafic–mafic host-rocks and was probably not transported over a great distance. The localization of Cu-for-Au replacement along primary gold – gangue grain boundaries, with an approach to pervasive replacement of thin stringer gold, indicates that fluid flow was channeled along pre-existing quartz–carbonate grain boundaries. Owing to the low sulfur fugacity in the fluid responsible for Au–Cu alloy mineralization, copper sulfides were unstable (note that pyrite and pyrrhotite are absent from the ore assemblage in the samples studied), and the lower thermodynamic activity of Cu in Au–Cu alloys, compared to native copper, permitted Cu to be precipitated in an alloy phase.

ACKNOWLEDGEMENTS

Samples investigated for this study were collected by J. Ploeger. We thank Yue Shao for translating Chen *et al.* (1982) into English, Yves Thibeau for assistance with EMPA, and Surface Science Western for use of XPS and SEM(EDX). Chris Stanley and Alan Criddle of the Natural History Museum, London, are thanked for their attempts to obtain reflectance data. Thanks are given to Drs. M. Novgorodova, E. Burke and Y. Moëlo for reviewing and editorial handling of this manuscript. This study was supported by a Natural Science and Engineering Research Council of Canada research grant to M.E.F.

REFERENCES

ANTUN, P., EL GORESY, A.E. & RAMDOHR, P. (1966): Ein neuartger Typ "hydrothermaler" Cu–Ni-Lagerstätten mit Bemerkungen über die Mineralien: Valleriit, Mackinawit, Oregonit. *Mineral. Deposita* **1**, 113-132.

AZAROFF, L.V. & BUERGER, M.J. (1958): *The Powder Method in X-Ray Crystallography.* McGraw-Hill, New York, N.Y.

BAIN, E.C. (1923): Crystal structure of solid solutions. *Trans. Am. Inst. Mining Engineers* **68**, 637-638.

BARRETT, C.S. & MASSALSKI, T.B. (1966): *Structure of Metals.* (3rd ed.) McGraw-Hill, New York, N.Y.

BATTERMAN, B.W. (1957): X-ray study of order in the alloy $CuAu_3$. *J. Appl. Phys.* **28**(5), 556-561.

BESSIÈRE, M., LEFEBVRE, S. & CALVAYRAC, Y. (1983): X-ray diffraction study of short-range order in a disordered Au_3Cu alloy. *Acta Crystallogr.* **B39**, 145-153.

BOYLE, R.W., BROWN, A.C., JOWETT, C.W. & KIRKHAM, R.V. (1989): Sediment-hosted stratiform copper deposits. *Geol. Assoc. Can., Spec. Pap.* **36**.

BRIGGS, D. & SEAH, M.P. (1985): *Practical Surface Analysis – by Auger and X-ray Photoelectron Spectroscopy.* Wiley, New York, N.Y.

BROWN, A.C. (1974) The copper province of northern Michigan, U.S.A. *In* Gisements Stratiformes et Provinces Cuprifères (P. Bartholomé, ed.). Société Géologique de Belgique, Liège, Belgique (317-330).

CASTELLANI, N.J. & LEROY, D.B. (1988): Final state core level binding energy shifts in binary alloys. *Z. Physik B: Condensed Matter* **71**, 315-319.

CHANNER, D.M.DER. & SPOONER, E.T.C. (1991): Multiple fluid-inclusion generations in variably deformed quartz: Hollinger-McIntyre and Kerr Addison – Chesterville Archean gold-bearing vein systems, northern Ontario. *Ont. Geol. Surv., Misc. Pap., Geoscience Research Grant Program, Summary of Research* 1990-91, 47-64.

CHEN, KEQIAO, YU, TINGGAO, ZHANG, YONGGE & PENG, ZHANG (1982): Tetra-auricupride, CuAu, discovered in China. *Scientia Geologica Sinica (Ti Chih Ko Hsueh/Dizhi Kexua)* **11**(1), 111-116 (in Chinese).

________, ________, ________ & ________ (1983): Tetra-auricupride, CuAu, discovered in China. *Am. Mineral.* **68**, 1250-1251 (English abstr.).

CRAIG, J.R. & VAUGHAN, D.J. (1981): *Ore Microscopy and Ore Petrography.* Wiley, New York, N.Y.

DOWNES, M.J. (1980): Structural and stratigraphic aspects of gold mineralization in the Larder Lake area, Ontario. *Ont. Geol. Surv., Misc. Pap.* **97**, 66-70.

GRATIAS, D., CONDAT, M. & FAYARD, M. (1972): I- and II-type superlattices in gold-rich copper–gold alloys. *Phys. Status Solidi* **A14**, 123-128.

HEYCOCK, C.T. & NEVILLE, F.H. (1897): Complete freezing point curves of binary alloys containing silver or copper together with another metal. *Phil. Trans., R. Soc. London* **A 189**, 25-69.

JAMES, W.F., BUFFAM, B.S.W. & COOPER, M.A. (1961): Report on geology and future exploration of Kerr Addison Gold Mines Ltd., McGarry Township, Ontario. Internal consultants' report, Kerr Addison Mines Ltd.

JOHANNSON, C.H. & LINDE, J.O. (1936): Röntgenographische und elektrische Untersuchungen des CuAu-systems *Ann. der Physik* **25**, 1-48.

JOHNSON, J.P. & MCCULLOCH, M.T. (1995): Sources of mineralising fluids for the Olympic Dam deposit (South Australia): Sm–Nd isotopic constraints. *Chem. Geol.* **121**, 177-199.

JORDAN, R.G., JIANG, Y., HOYLAND, M.A. & BEGLEY, A.M. (1991): Investigation of the electronic structure in Cu–Au I using X-ray photoelectron spectroscopy. *Phys. Rev. B* **43** (15), 12173-12175.

KERRICH, R. (1983): *Geochemistry of Gold Deposits in the Abitibi Greenstone Belt.* Special Volume 27, Canadian Institute of Mining & Metallurgy, Montreal, Quebec

KHAIN, V.E. (1985): *Geology of the U.S.S.R.* Gebrüder Borntraeger, Berlin, Germany.

KIRCHNER, F. (1922): Strukturuntersuchungen mit Röntgenstrahlen. *Ann. der Physik* **69**, 59-80.

KISHIDA, A. & KERRICH, R. (1987): Hydrothermal alteration zoning and gold concentration at the Kerr–Addison Archean lode gold deposit, Kirkland Lake, Ontario. *Econ. Geol.* **82**, 649-690.

KUBIAK, R. & JANCZAK, J. (1991) X-ray study of ordered phase formation in Au$_{31.6}$Cu$_{68.4}$, Au$_{50}$Cu$_{50}$, and Au$_{75}$Cu$_{25}$. *J. Alloys Compounds* **176**, 133-140.

LOZHECHKIN, M.P. (1939): New data on the chemical composition of "gold cupride". *Dokl. Akad. Nauk SSSR* **24**(5), 451-454 (in Russ.).

LU, S.S. & LIANG, C.K. (1966a): Existence of the CuAu$_3$ long range order in the Cu–Au system. *K'o Hsueh T'ung Pao* **17**(9), 395-396 (in Chinese).

________ & ________ (1966b): Experimental investigation of the second order order-disorder transformation. *K'o Hsueh T'ung Pao* **17**(11), 495-496 (in Chinese).

MATTHIESSEN, A. (1860): On the electrical conductivity of alloys. *Annals Phys. Chem.* **110** 190-221.

MOULDER, J.F., STICKLE, W.F., SOBOL, P.E. & BOMBEN, K.D. (1992): *Handbook of X-ray Photoelectron Spectroscopy.* Perkin Elmer Corp., Norwalk, Connecticut.

MURZIN, V.V. & SUSTAVOV, S.G. (1989): Solid phase transformations in natural copper-bearing gold. *Izvestiya Akademii Nauk SSSR seriya Geologicheskaya* **11**, 94-104 (in Russ.).

MYCROFT, J.R., BANCROFT, G.M., MCINTYRE, N.S. & LORIMER, J.W. (1995): Spontaneous deposition of gold on pyrite from solutions containing Au(III) and Au(I) chlorides. I. A surface study. *Geochim. Cosmochim. Acta* **59**, 3351-3365.

NOVGORODOVA, M.I. (1983): *Native Metals In Hydrothermal Ores.* Izd. Nauka, Moscow, Russia.

________ & TSEPIN, A.I. (1976): Phase composition of cupriferous gold. *Dokl. Acad. Sci. USSR* **227**(1), 121-123.

________, ________, GORSCHKOV, A.I., KUDREVA, I.M. & VALTCOV, N.V. (1977): New data on crystallochemistry and properties of natural intermetallic compounds of the Cu–Au system. *Zap. Vses. Mineral. Obshchest.* **106**(5), 540-552 (in Russ.).

OEN, I.S. & KIEFT, C. (1974): Nickeline with pyrrhotite and cubanite exsolution, Ni–Co rich loellingite and an Au–Cu alloy in Cr–Ni-ores from Beni Bousera, Morocco. *Neues Jahrb. Mineral., Monatsh.*, 1-8.

OKAMOTO, H., CHAKRABARTI, D.J., LAUGHLIN, D.E. & MASSALSKI, T.B. (1987): The Au–Cu (gold–copper) system. *Bull. Alloy Phase Diagrams* **8**(5), 454-474.

OKUZUMI, P.H., PERIO, P. & TOURNAIRE, M. (1959): Structure ordonnée d'un alliage de composition voisine de Au$_3$Cu. *Acta Crystallogr.* **12**, 1039-1043.

RAMDOHR, P. (1950): Neue Erzmineralien. *Fortschr. Mineral.* **28**, 69-70.

________ (1967): A widespread mineral association, connected with serpentinization. *Neues Jahrb. Mineral. Abh.* **107**, 241-265.

________ (1969): *The Ore Minerals and Their Intergrowths* (first ed.). Pergamon Press, Oxford, U.K.

________ (1980): *The Ore Minerals and Their Intergrowths* (second ed.). Pergamon Press, Oxford, U.K.

RAZIN, L.V., GOMONOVA, A.I., BYKOV, V.P. & MESHCHANKINA, V.I. (1971): A new natural mineral of gold, copper and palladium from the Talnakh deposit ores. *Zap. Vses. Mineral. Obshchest.* **100**, 66-76 (in Russ.).

ROSE, A.W. (1989): Mobility of copper and other heavy metals in sedimentary environments. *In* Sediment-Hosted Stratiform Copper Deposits (R.W. Boyle, A.C. Brown, C.W. Jowett & R.V. Kirkham, eds.). *Geol. Assoc. Can., Spec. Pap.* **36**. 97-110.

SCHWARTZ, M.O., AKANYANG, P., TRIPPLER, K. & NGWISANYI, T.H. (1995): The sediment-hosted Ngwako Pan copper deposit, Botswana. *Econ. Geol.* **90**, 1118-1147.

SMITH, J.P. & SPOONER, E.T.C., BROUGHTON, D.W. & PLOEGER, F.R. (1990): The Kerr Addison–Chesterville Archaean gold quartz vein system, Virginiatown: time sequence and associated mafic "albitite" dike swarm. *In* Geoscience Research Grant Program, Summary of Research 1989–90. *Ont. Geol. Surv., Misc. Pap.* **150**, 175-199.

________, ________, ________ & ________ (1993): Archean Au–Ag–(W) Quartz Vein/Disseminated Mineralization within the Larder Lake – Cadillac Break, Kerr Addison – Chesterville System, North East Ontario, Canada. *Ont. Geol. Surv., Open-File Rep.* **5831**.

________, ________ & Ploeger, F.R. (1991): The Kerr Addison/Chesterville Archean Au-quartz vein system, Virginiatown, N. Ontario. I. The bottom, and vertical trends. *Geol. Assoc. Can. – Mineral. Assoc. Can., Program Abstr.* **16**, A116.

Stumpfl, E.F. & Clark, A.M. (1965): Electron-probe micro-analysis of gold-platinoid concentrates from southeast Borneo. *Trans. Inst. Mining Metall.* **74**(708), B933-B946.

________ & ________ (1966): Electron probe microanalysis of gold-platinoid concentrates from southeast Borneo. Report of discussion at general meeting. *Trans. Inst. Mining Metall.* **75**, B97-B103.

Tihor, L.A. & Crocket, J.H. (1977): Gold distribution in the Kirkland Lake – Larder Lake area, with emphasis on Kerr Addison-type ore deposits – a progress report. *Geol. Surv. Can., Pap.* **77-1A**, 363-369.

Toth, R.S. & Sato, H. (1963): Antiphase domains in ordered Au_3Cu alloys. *J. Appl. Phys.* **35**, 698-703.

Tourigny, G., Doucet, D. & Bourget, A. (1993): Geology of the Bousquet 2 mine: an example of a deformed, gold-bearing, polymetallic sulfide deposit. *Econ. Geol.* **88**, 1578-1597.

Verryn, S.M.C., Merkle, R.K.W. & von Gruenewaldt, G. (1991): Gold- and associated ore minerals of the Waaikraal deposit, northwest of Brits, Bushveld Complex. *Eur. J. Mineral.* **3**, 451-466.

Warnick, M. (1981): *Gold Mineralization of the Flow Ores at Kerr Addison Mine.* B.Sc. thesis, Univ. Western Ontario, London, Ontario.

Yoshitake, M. & Yoshihara, K. (1991): Quantitative surface chemical analysis of Au–Cu alloys with XPS. *Surface Interface Anal.* **17**, 711-718.

Received July 30, 1996, revised manuscript accepted February 14, 1997.